

## **La clase pasada vimos:**

Heteroestructuras de semiconductores

Técnicas de crecimiento de cristales capa por capa

Ley de Vegard

Ingeniería de bandas:

Regla de Anderson

Tipos de alineación de bandas

Ejemplos de estructuras cuánticas

Barrera, pozo, doble barrera, superlattice

## **En esta clase veremos:**

Pozos cuánticos dobles y parabólicos

Aproximación de masa efectiva : una impureza

# Hetero-estructuras

## Regla de Anderson

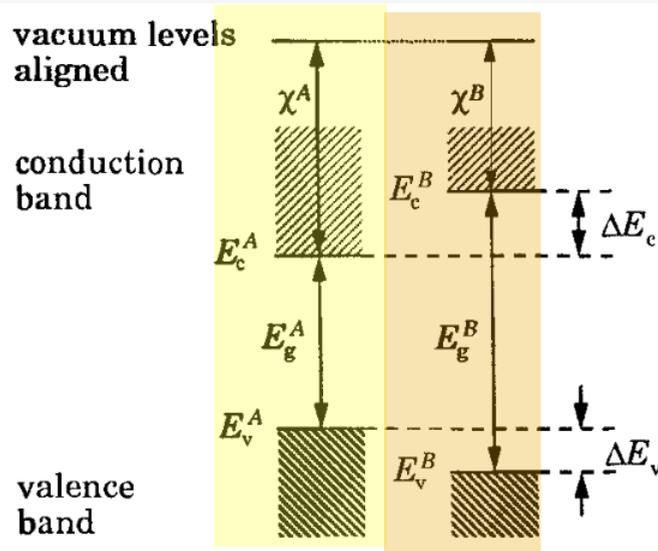
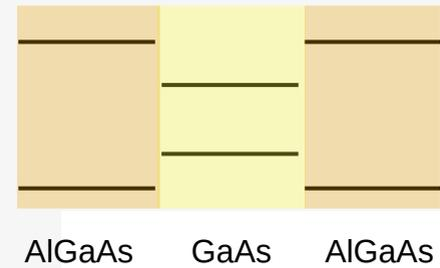


**FIGURE 3.4.** Anderson's rule for the alignment of the bands at a heterojunction between materials *A* and *B*, based on aligning the vacuum levels.

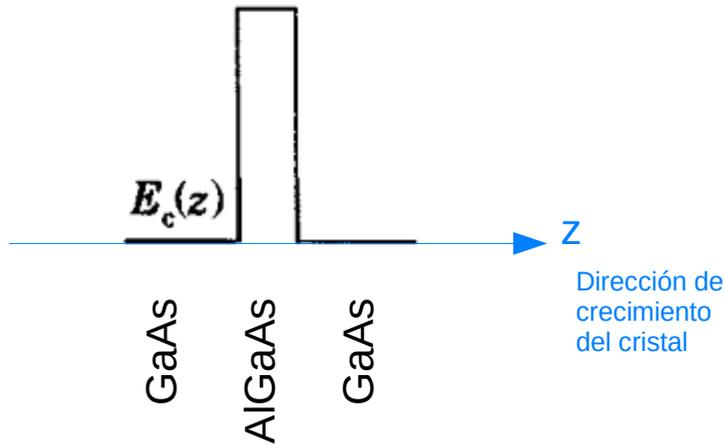
En un sandwich BAB se confinan en A tanto electrones como huecos



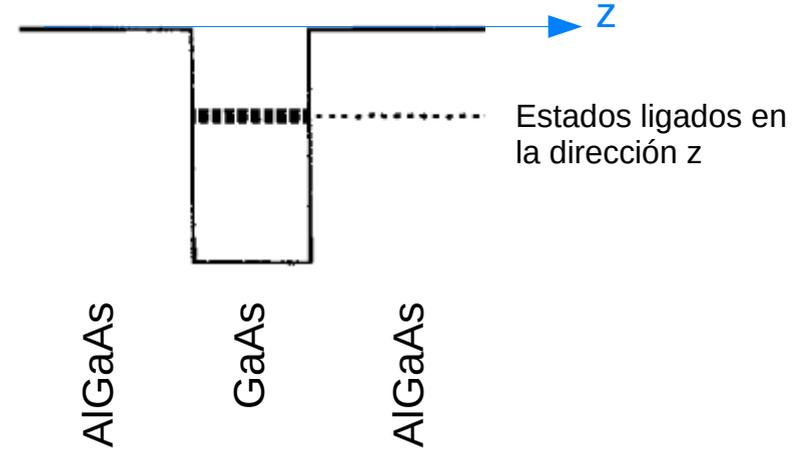
REPASO

# Ejemplos de estructuras cuánticas en capas

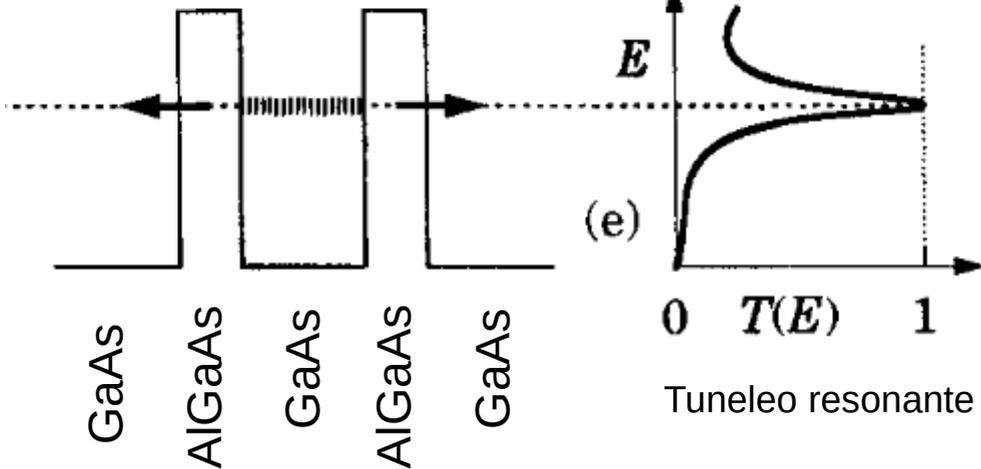
### Barrera túnel



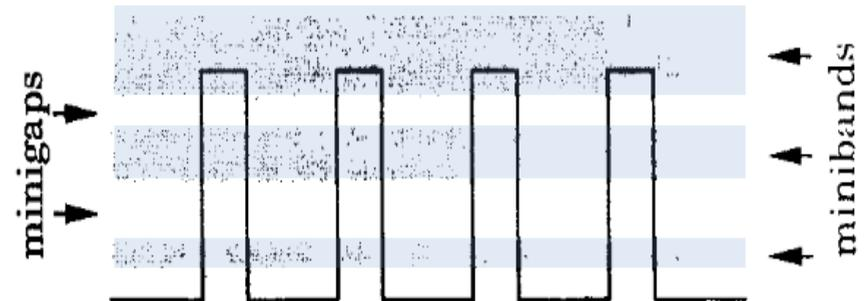
### Pozo cuántico



### Barrera doble

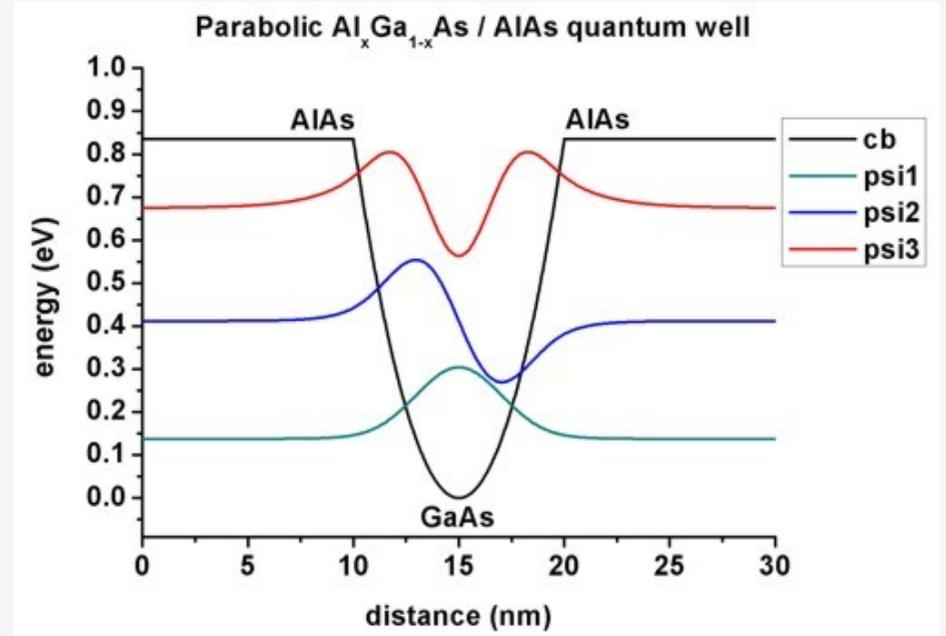
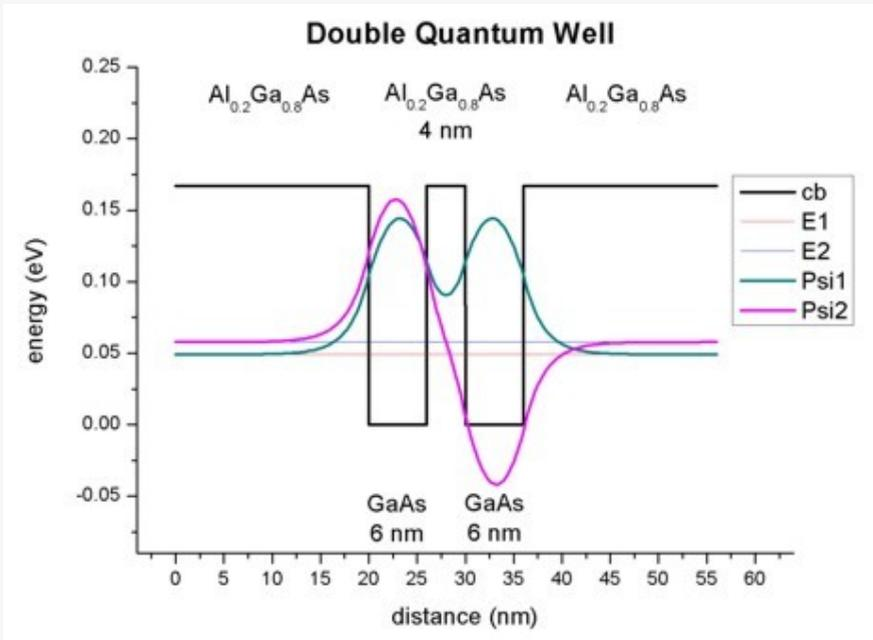


### Superlattice



Algunos ejemplos más de pozos cuánticos

# Pozos cuánticos dobles y parabólicos



# Pozos dobles

VOLUME 73, NUMBER 14

PHYSICAL REVIEW LETTERS

3 OCTOBER 1994

## Vertex-Correction-Driven Intersubband Spin-Density Excitonic Instability in Double Quantum Well Structures

S. Das Sarma and P. I. Tamborenea

Department of Physics, University of Maryland, College Park, Maryland 20742-4111

(Received 15 March 1994)

We show that exchange-correlation induced many-body excitonic vertex correction may lead to an instability in the normal ground state of a semiconductor double quantum well structure by suppressing the symmetric-antisymmetric intersubband gap at low but accessible ( $\sim 0.7 \times 10^{11} \text{ cm}^{-2}$ ) electron densities. We predict as a consequence a novel electronic phase transition where the lowest intersubband spin-density-excitation gap vanishes giving rise to a new many-body triplet excitonic liquid ground state which is more stable at low densities than the usual two dimensional Fermi liquid phase.

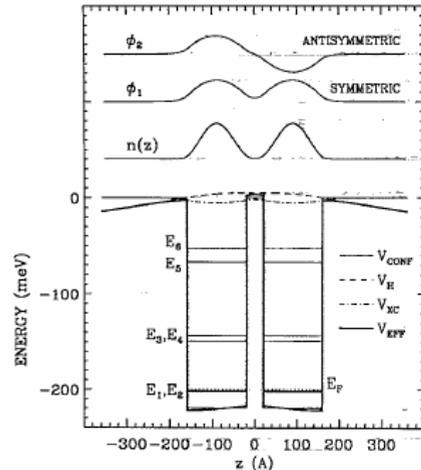


FIG. 1. The typical double quantum well structure ( $N_s = 10^{11} \text{ cm}^{-2}$ ) with the self-consistent local-density-approximation calculated energy levels and wave functions for the symmetric-antisymmetric levels. The bare ( $V_{\text{conf}}$ ), Hartree ( $V_H$ ), and exchange-correlation ( $V_{\text{xc}}$ ) contributions to the effective potential ( $V_{\text{eff}}$ ) are shown. (The SAS gap  $\Delta_{\text{SAS}} = |E_2 - E_1|$ .)

# Pozos parabólicos con imperfecciones

PHYSICAL REVIEW B

VOLUME 49, NUMBER 23

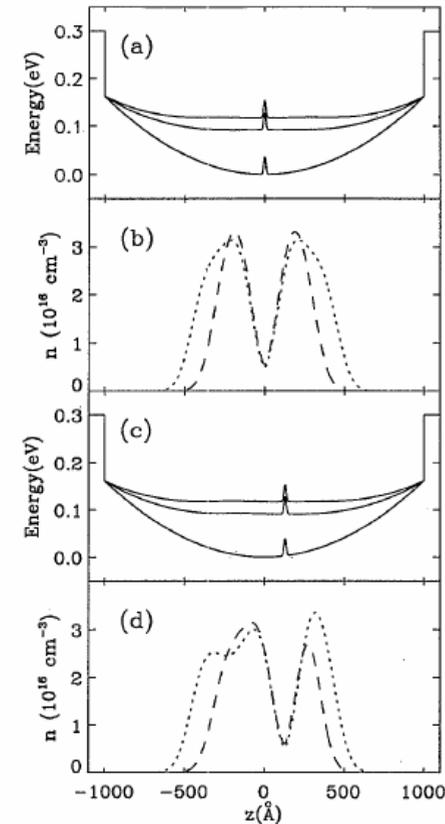
15 JUNE 1994-I

## Collective excitations in imperfect parabolic quantum wells with in-plane magnetic fields

P. I. Tamborenea and S. Das Sarma

Department of Physics, University of Maryland, College Park, Maryland 20742-4111

(Received 7 July 1993; revised manuscript received 25 January 1994)



# Pozos parabólicos asimétricos, con dos curvaturas diferentes



Solid State Communications, Vol. 89, No. 12, pp. 1009-1012, 1994

Elsevier Science Ltd

Printed in Great Britain. All rights reserved

0038-1098/94 \$6.00+.00

0038-1098(94)(E0095-S

## COLLECTIVE EXCITATIONS IN ASYMMETRIC PARABOLIC QUANTUM WELLS

P. I. Tamborenea and S. Das Sarma  
Department of Physics, University of Maryland,  
College Park, Maryland 20742, USA

(Received 12 January 1994 by A. Pinczuk)

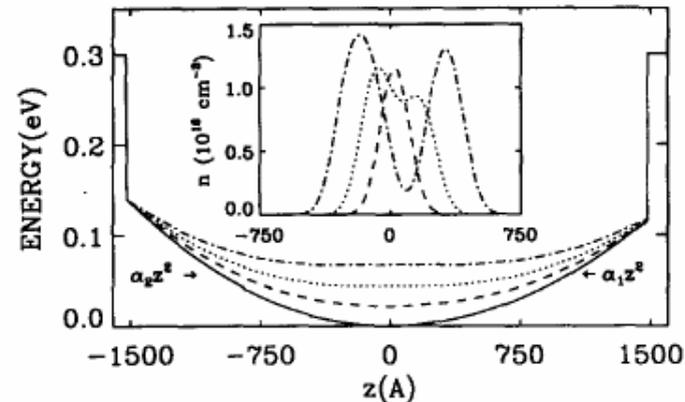


Fig. 1. Model bare potential of the asymmetric parabolic well (solid line), and calculated self-consistent potentials with an in-plane magnetic field of  $B = 5.8 T$ , for  $N_s = 2.4$  (dash line),  $4.7$  (dotted line), and  $7.5 \times 10^{10} \text{ cm}^{-2}$  (dash-dot line); inset: corresponding calculated self-consistent densities.

Aproximación de masa efectiva

# Aproximación de masa efectiva

Supongamos que se agrega al material algo nanométrico que perturba su periodicidad, por ejemplo, una impureza:

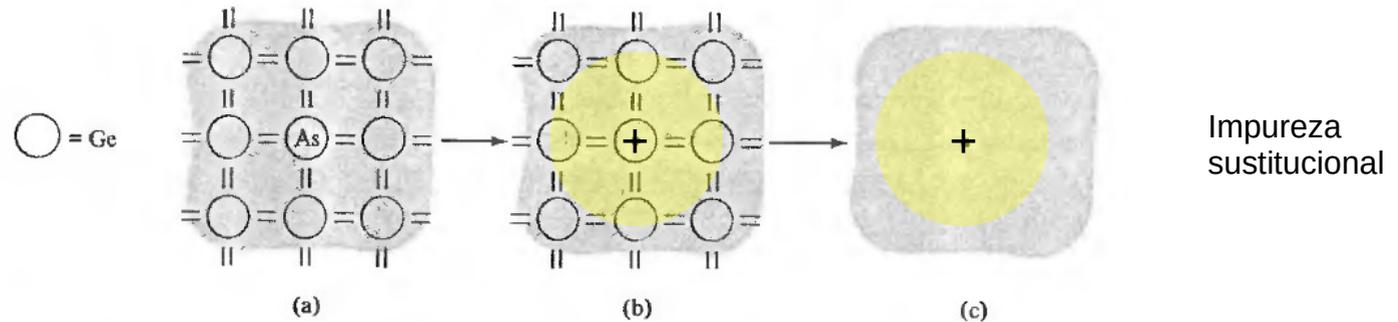


Figure 28.11

(a) Schematic representation of a substitutional arsenic (valence 5) donor impurity in a germanium (valence 4) crystal. (b) The arsenic (As) can be represented as a germanium atom *plus* an additional unit of positive charge fixed at the site of the atom (circled dot). (c) In the semiclassical approximation, in which the pure semiconductor is treated as a homogeneous medium, the arsenic impurity is represented as a fixed point charge  $+e$  (dot).

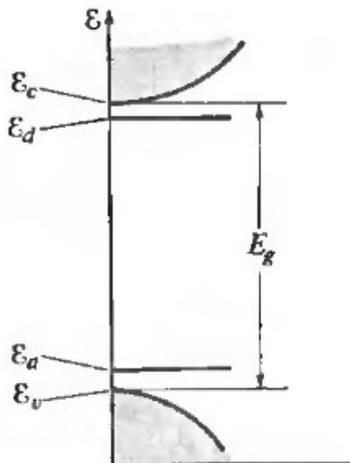
# Aproximación de masa efectiva

Ecuación de Schrödinger para el electrón donado al material:

$$[\hat{H}_{\text{per}} + V_{\text{imp}}(\mathbf{R})]\psi(\mathbf{R}) = E\psi(\mathbf{R})$$

Queremos ver como se llega a un modelo simplificado sin  $H_{\text{per}}$

En el problema de la impureza sustitucional se llega a un problema equivalente al átomo de hidrógeno con *constante dieléctrica* y *masa efectiva*:



$$\left[ -\frac{\hbar^2 \nabla^2}{2m^*} - \frac{e^2}{\epsilon r} \right] \psi(\mathbf{r}) = E^* \psi(\mathbf{r})$$

Ecuación de Schrödinger efectiva

$$r_0 = \frac{m}{m^*} \epsilon a_0$$

radio de Bohr efectivo (decenas de angstroms)

$$\epsilon = \frac{m^*}{m} \frac{1}{\epsilon^2} \times 13.6 \text{ eV}$$

Rydberg efectivo (meV)

(5 meV en GaAs)

# Aproximación de masa efectiva

Estados de Bloch y energías del cristal puro:  $\hat{H}_{\text{per}}\phi_{nk}(x) = \varepsilon_n(k)\phi_{nk}(x)$

Expandimos el estado del electrón con la impureza presente :

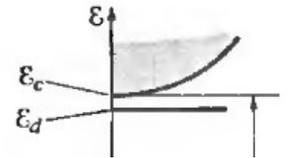
$$\psi(x) = \sum_n \int_{-\pi/a}^{\pi/a} \tilde{\chi}_n(k) \phi_{nk}(x) \frac{dk}{2\pi}$$

Coeficientes de la expansión

Aproximaciones :

(1) Una sola banda, por ejemplo banda de conducción  
(un solo  $n$  en la suma)

(2) Integrar  $k$  cerca del mínimo



## Aproximación de masa efectiva

$$\psi(x) = \sum_n \int_{-\pi/a}^{\pi/a} \tilde{\chi}_n(k) \phi_{nk}(x) \frac{dk}{2\pi}$$

(2) Integrar  $k$  cerca del mínimo :

Aproximamos la función de Bloch cerca de  $k = 0$  :

$$\phi_{nk}(x) = u_{nk}(x) e^{ikx} \approx u_{n0}(x) e^{ikx} = \phi_{n0}(x) e^{ikx}$$

$$\longrightarrow \psi(x) \approx \phi_{n0}(x) \int_{-\pi/a}^{\pi/a} \tilde{\chi}(k) \exp(ikx) \frac{dk}{2\pi} = \phi_{n0}(x) \chi(x)$$

## Aproximación de masa efectiva

$$\psi(x) \approx \phi_{n0}(x) \int_{-\pi/a}^{\pi/a} \tilde{\chi}(k) \exp(ikx) \frac{dk}{2\pi} = \phi_{n0}(x) \chi(x)$$

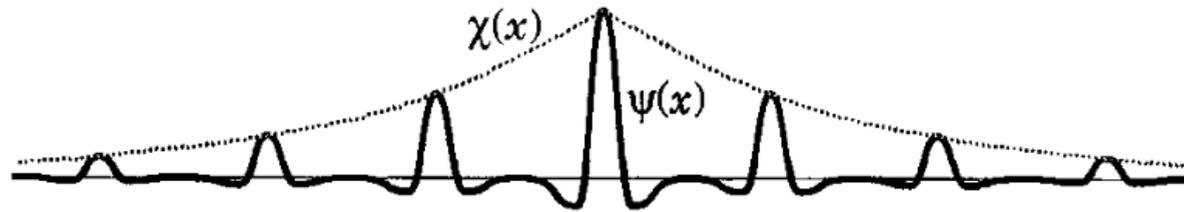


**FIGURE 3.21.** Wave function around an impurity, showing the envelope function  $\chi(x)$  that modulates the Bloch function to give the full wave function  $\psi(x)$ .

La función envolvente contiene valores chicos de  $k$  en su expansión de Fourier, por lo tanto es **suave** comparada con el parámetro de red

Vamos a ver que en este caso es el ground state hidrogenoide:  $\chi(r) \sim e^{-r/a_0^*}$

## Aproximación de masa efectiva

Falta obtener la ecuación para la función envolvente. Teníamos el problema exacto:

$$\left\{ \begin{array}{l} [\hat{H}_{\text{per}} + V_{\text{imp}}(\mathbf{R})]\psi(\mathbf{R}) = E\psi(\mathbf{R}) \\ \psi(x) = \sum_n \int_{-\pi/a}^{\pi/a} \tilde{\chi}_n(k) \phi_{nk}(x) \frac{dk}{2\pi} \end{array} \right.$$

Nos quedamos con una sola banda en la expansión:

$$\begin{aligned} \hat{H}_{\text{per}}\psi(x) &= \hat{H}_{\text{per}} \int_{-\pi/a}^{\pi/a} \tilde{\chi}(k) \phi_{nk}(x) \frac{dk}{2\pi} = \int_{-\pi/a}^{\pi/a} \tilde{\chi}(k) \varepsilon_n(k) \phi_{nk}(x) \frac{dk}{2\pi} \\ &\approx \phi_{n0}(x) \int_{-\pi/a}^{\pi/a} \tilde{\chi}(k) \varepsilon_n(k) e^{ikx} \frac{dk}{2\pi}. \end{aligned}$$

## Aproximación de masa efectiva

Supongamos que:  $\varepsilon_n(k) = \sum_m a_m k^m$

Reemplazando:

$$\hat{H}_{\text{per}} \psi(x) \approx \phi_{n0}(x) \int_{-\pi/a}^{\pi/a} \tilde{\chi}(k) \varepsilon_n(k) e^{ikx} \frac{dk}{2\pi}$$

$$\approx \phi_{n0}(x) \sum_m a_m \int_{-\pi/a}^{\pi/a} \tilde{\chi}(k) k^m e^{ikx} \frac{dk}{2\pi}$$

$$\approx \phi_{n0}(x) \sum_m a_m \left(-i \frac{d}{dx}\right)^m \chi(x)$$

$$\equiv \phi_{n0}(x) \varepsilon_n \left(-i \frac{d}{dx}\right) \chi(x)$$

Integración por partes  
y transf. de Fourier

## Aproximación de masa efectiva

Entonces obtuvimos: 
$$\left[ \varepsilon_n \left( -i \frac{d}{dx} \right) + V_{\text{imp}}(x) \right] \chi(x) = E \chi(x).$$

Ecuación de Schrödinger efectiva para la función envolvente

In 3D: 
$$\varepsilon_n(-i d/dx) \longrightarrow \varepsilon_n(-i \nabla)$$

Cerca del mínimo de la banda de conducción:

$$\varepsilon_n(\mathbf{K}) \approx E_c + \frac{\hbar^2 K^2}{2m_0 m_e} \longrightarrow \varepsilon_n(-i \nabla) \approx E_c - \frac{\hbar^2}{2m_0 m_e} \nabla^2$$

$$\longrightarrow \left[ -\frac{\hbar^2}{2m_0 m_e} \nabla^2 + V_{\text{imp}}(\mathbf{R}) \right] \chi(\mathbf{R}) = (E - E_c) \chi(\mathbf{R})$$

# Aproximación de masa efectiva

Incluyendo el potencial de la impureza ionizada:

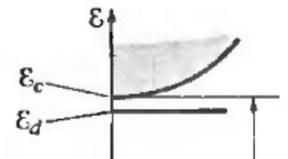
$$\left( -\frac{\hbar^2}{2m_0m_e} \nabla^2 - \frac{e^2}{4\pi\epsilon_0\epsilon_b R} \right) \chi(\mathbf{R}) = (E - E_c) \chi(\mathbf{R})$$

$\chi(R) = (\pi a_B^3)^{-1/2} \exp(-R/a_B)$ , where  $a_B$  is the *Bohr radius*

$$\mathcal{R} = \left( \frac{e^2}{4\pi\epsilon} \right)^2 \frac{m}{2\hbar^2} = \frac{\hbar^2}{2ma_B^2} = \frac{1}{2} \frac{e^2}{4\pi\epsilon a_B}$$

$$a_B = \frac{4\pi\epsilon\hbar^2}{me^2}$$

$\mathcal{R} \approx 5 \text{ meV}$  and  $a_B \approx 10 \text{ nm}$  for electrons in GaAs

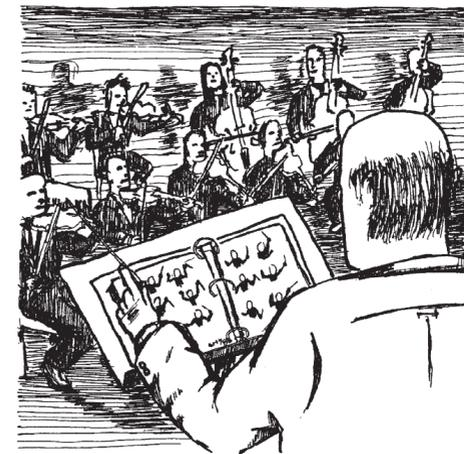


The lowest state has a binding energy of  $4\mathcal{R}$ , four times larger than the corresponding three-dimensional result. This is particularly important for an *exciton*, an

# Fundamentals of Semiconductors

Physics and Materials Properties

4.2	Shallow or Hydrogenic Impurities .....	161
4.2.1	Effective Mass Approximation .....	162
4.2.2	Hydrogenic or Shallow Donors .....	166



A SEMI-CONDUCTOR

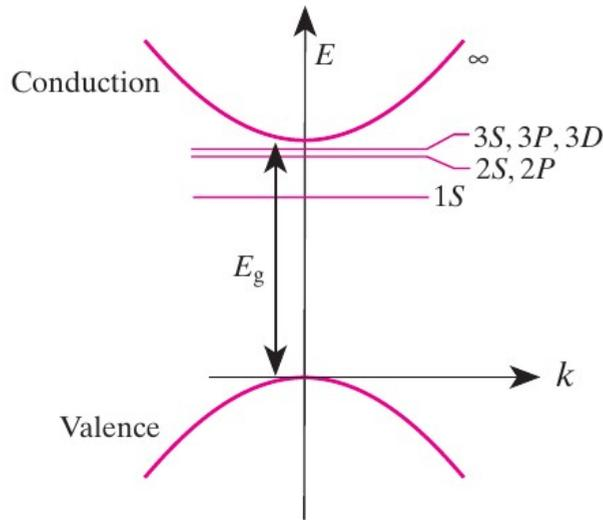


**Fig. 4.1.** Schematic diagram of the  $n=1$ , 2, and 3 bound states of a shallow donor electron near a nondegenerate and parabolic conduction band (corresponding to  $n = \infty$ ).  $E_g$  is the bandgap

## Aproximación de masa efectiva

**Table 4.1.** Experimental binding energies of the 1s state of shallow donors in some zinc-blende-type semiconductors (from [Ref. 4.4, p. 224]) compared with the predictions of (4.24)

Semiconductor	Binding energy from (4.24) [meV]	Experimental binding energy of common donors [meV]
GaAs	5.72	Si <sub>Ga</sub> (5.84); Ge <sub>Ga</sub> (5.88) S <sub>As</sub> (5.87); Se <sub>As</sub> (5.79)
InP	7.14	7.14
InSb	0.6	Te <sub>Sb</sub> (0.6)
CdTe	11.6	In <sub>Cd</sub> (14); Al <sub>Cd</sub> (14)
ZnSe	25.7	Al <sub>Zn</sub> (26.3); Ga <sub>Zn</sub> (27.9) F <sub>Se</sub> (29.3); Cl <sub>Se</sub> (26.9)

$$R = \left( \frac{m^*}{m_0} \right) \left( \frac{1}{\epsilon_0^2} \right) \left( \frac{e^4 m_0}{2\hbar^2} \right) \frac{1}{(4\pi\epsilon_0)^2}, \quad (4.24)$$

## Resumen de la clase 6

Pozos cuánticos dobles y parabólicos

Aproximación de masa efectiva : una impureza